Available online at www.sciencedirect.com
SCIENCE DIRECT®
Optics Communications 255 (2005) 23–34
OPTICS COMMUNICATIONS
www.elsevier.com/locate/optcom

Spectral modification by line singularity in Fresnel diffraction from 1D phase step

M.T. Tavassoly [a,b,*], M. Amiri [b,c], E. Karimi [b], H.R. Khalesifard [b]

[a] Physics Department, Tehran University, Kargar Shomally, Tehran 14394, Iran
[b] Institute for Advanced Studies in Basic Sciences (IASBS), Gava Zang, Zanjan 45195, Iran
[c] Physics Department, Bu-Ali Sina University, Hamadan 65178, Iran

Received 30 September 2004; received in revised form 16 May 2005; accepted 1 June 2005

Abstract

In this work, we show when a coherent beam of light diffracts from a 1D phase step of specified height, phase singularity appears in the diffracted field. By changing the height of the step, singularities for different frequencies or wavelengths are formed which modify the spectrum of the incident beam differently. We have calculated the modifying factor and simulated the modified spectral profiles for different singularities at points in the neighborhoods of the singularities for two different sources used in the experimental studies. In the latter studies, using a monochromator, we have specified the spectral profiles at points in the neighborhoods of the singularities. The simulation and experimental results are in very good agreement. Further development of the work and its potential applications are also discussed.

PACS: 42.25.F; 33.70.J

Keywords: Fresnel diffraction; Spectral modification; Line singularity; Phase step

1. Introduction

In recent years a great deal of work has been done on the structure of optical fields in the neighborhood of phase singularities. The subject is rich and interesting, and it is growing as a new branch of physical optics [1–3]. The majority of works in this area deal with spatially fully coherent monochromatic optical fields, but, very recently polychromatic and partially coherent fields also have been considered which reveal remarkable features [4–8]. In a report, Gbur, Visser, and Wolf (GVW) [4,5] have shown that the spectral profile of a coherent polychromatic converging spherical wave at points in the neighborhood of a phase singularity, a point with zero amplitude for a particular

* Corresponding author. Tel.: +98 218258576; fax: +98 218004781.
E-mail address: tavasoli@iasbs.ac.ir (M.T. Tavassoly).

0030-4018/$ - see front matter © 2005 Elsevier B.V. All rights reserved.
doi:10.1016/j.optcom.2005.06.048

spectral component, experiences drastic changes, like splitting, blue shifting, and red shifting. In fact, GVW have applied the Huygens–Fresnel principle in paraxial domain to calculate the intensity distribution, due to a converging spherical coherent polychromatic wave of a given spectral profile, at points in the neighborhood of the geometrical focus. They have derived a spectral modifying factor which depends on the geometry of the wave and wavelength. Following GVW, Berry [6,7] has shown that, for illumination with white light, the spectrum near a typical isolated phase singularity can be described by a universal function of position and he has predicted the appearance of the singularity to human eyes. Following the latter theoretical works, Popescu and Dogariu [9], using high resolution interferometric technique have reported the experimental observation of the anomalous spectral behavior predicted by GVW.

In this report, we show when a plane or cylindrical monochromatic wavefront diffracts from a 1D phase step, line singularities occur for particular heights of the step. By increasing the height of the step one can increase the wavelength of the singularity. For polychromatic illumination the spectral profile of the diffracted field in the neighborhood of a singularity is modified in agreement with GVW's predictions and the modifying factor strongly depends on the step height and the distance from the singularity plane. The modifying factor is calculated and, using the spectral profiles of the sources used in the experimental study, the spectral profiles of the diffracted field at points in the neighborhoods of different singularities are simulated. In experimental study the phase step, formed by two optically flat blocks, is illuminated by spatially coherent white light, with and without a broad band transmission filter, and the spectra of the diffracted field at different distances from the singularity plane on both sides are specified for different singularities.

The report is organized as follows. In Section 2, we present a brief review of the Fresnel diffraction (FD) from 1D phase step and calculate the spectral modifying factor. Experimental procedure, results, and, their corresponding simulations are included in Section 3. Concluding remarks and further development of the study are presented in Section 4.

2. Fresnel diffraction from 1D phase step

In Fig. 1, a cylindrical wavefront originating from a linear source illuminates a 1D step of height h. The linear source and the edge of the step are perpendicular to the page. (The arrangement of the set-up is so that there is no direct light propagation from the source to the screen.) Applying

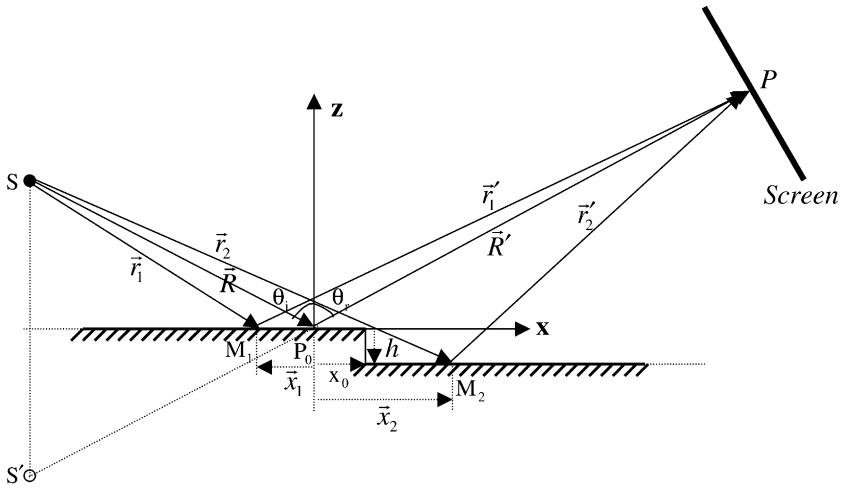

Fig. 1. The geometry used for calculating the Fresnel–Kirchhoff integral and the spectral modifying factor for 1D phase step.

the Fresnel–Kirchhoff integral we calculate the diffracted complex amplitude at point P on a screen perpendicular to the reflected ray passing through point P. We denote the optical disturbance by

$$V(\vec{r},t) = U(\vec{r},\lambda)\mathrm{e}^{-\mathrm{i}\omega t}, \tag{1}$$

where,

$$U(\vec{r},\lambda) = \frac{A(\lambda)}{\sqrt{r}}\mathrm{e}^{\mathrm{i}kr}, \tag{2}$$

is the complex amplitude of the wave at distance r from the source for wavelength λ and k is the wavenumber. Considering Fig. 1 the Fresnel–Kirchhoff integral for point P at the distance $R+R'$ from the image of the source, S', takes the following form:

$$U(R,R',\lambda) = \sqrt{\frac{-\mathrm{i}}{\lambda}}\left[\int_{-\infty}^{x_0}\frac{A(\lambda)}{\sqrt{r_1 r_1'}}\mathrm{e}^{\mathrm{i}k(r_1+r_1')}\,\mathrm{d}x + \int_{x_0}^{+\infty}\frac{A(\lambda)}{\sqrt{r_2 r_2'}}\mathrm{e}^{\mathrm{i}k(r_2+r_2')}\,\mathrm{d}x\right], \tag{3}$$

where $\sqrt{\frac{-\mathrm{i}}{\lambda}}$ is the inclination factor for cylindrical wave (see Appendix A) and x_0 is the distance of the intersection point of the line $S'P$ with the reflecting surface, P_0 in Fig. 1, from the step edge. Now, according to Fig. 1 we have

$$\begin{aligned}\vec{r}_1 &= \vec{R} + \vec{x}_1,\\ \vec{r}_1' &= \vec{R}' - \vec{x}_1,\end{aligned} \tag{4}$$

in the first integrand, and

$$\begin{aligned}\vec{r}_2 &= \vec{R} + \vec{h} + \vec{x}_2,\\ \vec{r}_2' &= \vec{R}' - \vec{h} - \vec{x}_2,\end{aligned} \tag{5}$$

in the second integrand.

In FD approximation, where $|\vec{R}|$ and $|\vec{R}'|$ are very large compared with the other terms, Eq. (4) for $x_1 = x$ leads to the following:

$$\begin{aligned}r_1 &\simeq R + \frac{x^2}{2R} - x\sin\theta_\mathrm{i},\\ r_1' &\simeq R' + \frac{x^2}{2R'} + x\sin\theta_\mathrm{r},\end{aligned} \tag{6}$$

where θ_i and θ_r are incidence and reflection angles at point P_0, respectively. By similar consideration, Eq. (5) for $x_2 = x$ leads to

$$\begin{aligned}r_2 &\simeq R + \frac{x^2}{2R} + x\sin\theta_\mathrm{i} + h\cos\theta_\mathrm{i} + \frac{h^2}{2R},\\ r_2' &\simeq R' + \frac{x^2}{2R'} - x\sin\theta_\mathrm{r} + h\cos\theta_\mathrm{r} + \frac{h^2}{2R'},\end{aligned} \tag{7}$$

substituting from Eqs. (6) and (7) in Eq. (3) and ignoring very small terms $h^2/2R$ and $h^2/2R'$, and recalling that $\theta_\mathrm{i} = \theta_\mathrm{r}$, we get

$$U(R,R',\lambda) = \sqrt{\frac{-\mathrm{i}}{\lambda}}\frac{A(\lambda)\mathrm{e}^{\mathrm{i}k(R+R')}}{\sqrt{RR'}}\left[\int_{-\infty}^{x_0}\mathrm{e}^{\mathrm{i}\frac{kx^2}{2}\left(\frac{1}{R}+\frac{1}{R'}\right)}\,\mathrm{d}x + \mathrm{e}^{\mathrm{i}2kh\cos\theta_\mathrm{i}}\int_{x_0}^{+\infty}\mathrm{e}^{\mathrm{i}\frac{kx^2}{2}\left(\frac{1}{R}+\frac{1}{R'}\right)}\,\mathrm{d}x\right]. \tag{8}$$

In deriving Eq. (8) we have also ignored amplitude changes due to variation of r_1, r_2, and r_1', r_2' under the root square sign in Eq. (3) and have equated them by R and R', respectively.

Eq. (8) reveals interesting features. For example, for $2h\cos\theta_\mathrm{i} = m\lambda$, $(m = 0, \pm1, \pm2, \ldots)$ the step is not felt and the system behaves like a very wide slit or mirror. For $x_0 = 0$, and $2h\cos\theta_\mathrm{i} = (2m+1)\lambda/2$, we have $U(R,R',\lambda) = 0$ and the intensity at the field points corresponding to the step edge becomes zero. Therefore, we have line singularity, and by changing the height of the step, one can produce singularities for different wavelengths. For large x_0, the contribution of the second integral is negligible.

In order to evaluate the intensity distribution on the screen we introduce the following abbreviations:

$$\begin{aligned}&kx^2\left(\frac{1}{R}+\frac{1}{R'}\right) = \pi v^2,\\ &2kh\cos\theta_\mathrm{i} = \Phi,\\ &\frac{\mathrm{e}^{\mathrm{i}k(R+R')}}{\sqrt{R+R'}} = U_0\end{aligned} \tag{9}$$

and in Eq. (8) we express x in term of v, which is referred to as the normalized distance, to get the following more compact expression:

$$U(R,R',\lambda) = \sqrt{\frac{-\mathrm{i}}{2}}A(\lambda)U_0\left[\int_{-\infty}^{v_0}\mathrm{e}^{\mathrm{i}\frac{\pi v^2}{2}}\,\mathrm{d}v + \mathrm{e}^{\mathrm{i}\Phi}\int_{v_0}^{+\infty}\mathrm{e}^{\mathrm{i}\frac{\pi v^2}{2}}\,\mathrm{d}v\right], \tag{10}$$

where, v_0 is the normalized distance corresponding to x_0. Now, we denote the disturbance $U(R,R',\lambda)$

for points like P_0, lying on the left side of the step edge, by U_L and for the corresponding points on the right side by U_R. Thus, Eq. (10) takes one of the following forms:

$$U_L = K'\left[\int_{-\infty}^{v_L} e^{i\frac{\pi v^2}{2}}\,dv + e^{i\Phi}\int_{v_L}^{+\infty} e^{i\frac{\pi v^2}{2}}\,dv\right], \tag{11}$$

or

$$U_R = K'\left[\int_{-\infty}^{-v_R} e^{i\frac{\pi v^2}{2}}\,dv + e^{i\Phi}\int_{-v_R}^{+\infty} e^{i\frac{\pi v^2}{2}}\,dv\right], \tag{12}$$

where K' stands for $\sqrt{\frac{-i}{2}}A(\lambda)U_0$ and v_L or v_R represents v_0 for the left or the right side of the step edge. Considering that the Fresnel integrand is an even function, that is; $\int_{-v}^{0}\ldots dv = \int_{0}^{v}\ldots dv$, we can write

$$U_L = K'\left[(1+e^{i\Phi})\int_0^{+\infty} e^{i\frac{\pi v^2}{2}}\,dv + (1-e^{i\Phi})\int_0^{v_L} e^{i\frac{\pi v^2}{2}}\,dv\right]. \tag{13}$$

Finally, substituting [10]

$$\int_0^{+\infty} e^{i\frac{\pi v^2}{2}}\,dv = \frac{1}{2}(1+i) \tag{14}$$

and

$$\int_0^{v_L} e^{i\frac{\pi v^2}{2}}\,dv = (C_L + iS_L), \tag{15}$$

in Eq. (13) we reach at

$$U_L = K'\left[\frac{1}{2}(1+e^{i\Phi})(1+i) + (1-e^{i\Phi})(C_L+iS_L)\right]. \tag{16}$$

Multiplying U_L by its complex conjugate and replacing K' and U_0 by the given values, we get the required intensity

$$I_L = \frac{I_0(\lambda)}{(R+R')}\left[\cos^2(\Phi/2) + 2(C_L^2+S_L^2)\sin^2(\Phi/2) - (C_L - S_L)\sin(\Phi)\right], \tag{17}$$

where $I_0(\lambda) = A^2(\lambda)$ is the source spectral function. Similar operations on the right hand side disturbance U_R lead to

$$I_R = \frac{I_0(\lambda)}{(R+R')}\left[\cos^2(\Phi/2) + 2(C_R^2+S_R^2)\sin^2(\Phi/2) + (C_R - S_R)\sin(\Phi)\right]. \tag{18}$$

Now, we divide the both sides of Eqs. (17) and (18) by $\frac{I_0(\lambda_0)}{(R+R')}$, the intensity of the central wavelength of the source spectrum λ_0 at the observation point, to get the normalized intensity distributions

$$I_{LN} = \frac{I_0(\lambda)}{I_0(\lambda_0)}M_L \tag{19}$$

and

$$I_{RN} = \frac{I_0(\lambda)}{I_0(\lambda_0)}M_R, \tag{20}$$

where

$$M_L = \left[\cos^2(\Phi/2) + 2(C_L^2+S_L^2)\sin^2(\Phi/2) - (C_L - S_L)\sin(\Phi)\right] \tag{21}$$

and

$$M_R = \left[\cos^2(\Phi/2) + 2(C_R^2+S_R^2)\sin^2(\Phi/2) + (C_R - S_R)\sin(\Phi)\right], \tag{22}$$

are spectral modifying factors for the left and the right sides of the edge. The modifying factors obtained, depend on the ratio of the step height to the wavelength, which is included in phase Φ, the distance from the step edge, and the wavelength which are included in C and S. They are not equal in general, and the difference is more pronounced for considerable $|C-S|$, that is; for points corresponding to the neighborhood of the step edge. Thus, the spectral distributions on both sides of the edge are different except at points for which $C = S$.

3. Simulation and experimental studies

In order to study the effect of the modifying factor derived in Section 2 experimentally, the following experiments are designed and carried out. A white light source (XENOPHOT HLX 64640 FCS 24V-150W) illuminates a narrow slit of width 0.07 mm. The transmitted light strikes the vertical surfaces of two rectangle blocks of glass, one mounted on the top of the other (Fig. 2).

The surfaces of the blocks facing the light are optically flat and coated with aluminum to enhance the reflectance. One of the blocks can be displaced horizontally with respect to the other

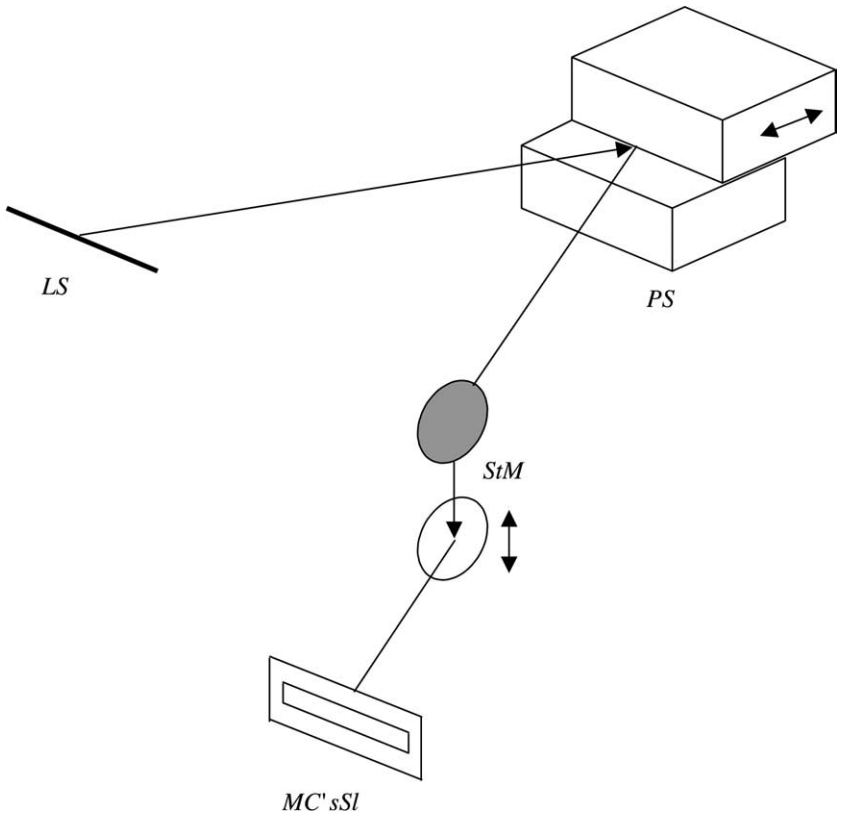

Fig. 2. The sketch of the main part of the setup used to study the spectral modification of the light diffracted from 1D phase step. The abbreviations LS, PS, StM, and MC's Sl stand for: linear source, phase step, steering mirrors, and monochromator's slit, respectively.

to produce phase step with the desired height. The distance between the source slit and the phase step is made large – 235 cm – to provide illumination of high spatial coherency. The light incident angle on the step is about 5° and the diffracted light strikes perpendicularly the entrance slit of a monochromator (MC) which is located at the distance 730 cm from the phase step. Instead of scanning the diffracted light distribution by the entrance slit of the MC, a steering mirrors device, which consists of two parallel mirrors mounted on a vertical stand is installed in the path of the diffracted beam, StM in Fig. 2. By moving one of the mirrors in vertical direction, different sections of the beam profile face the entrance slit of the MC and this guarantees similar illuminations of MC by different beam sections. The width of the entrance slit is 0.12 mm (at observation screen) which corresponds to $\Delta v \simeq 0.04$ on the Cornu spiral. The arrangement of the setup is so that the intensity distribution in term of v in the range -0.16 to $+0.16$ corresponds to the neighborhood of the step edge in the range of -0.112 to $+0.112$ mm. Thus, one can study the spectral profiles of the diffracted beam at small intervals at points very close to the phase singularity. The width of the MC's exit slit is also 0.12 mm, and it faces a PMT (Type 9558B from Electron Tubes Co.). The resolution of MC is 0.1 nm, but the data are registered at 5 nm intervals. To change the height of the phase step, one of the blocks is displaced by using micropositioner equipped with Piezoelectric elements and the amount of the displacement is controlled by an interferometer. Two series of experiments are carried out. In the first series, two color filters (Filter No. 3387 es3–72–3.0 mm and filter No. 5031 es5–56–4.63 mm from Corning Co.) are put together and is installed in front of the white light source

to apodize the tails of the spectrum. In the second series the filters are removed. For recording the diffracted light spectra corresponding to the points on the left and on the right sides of the step edge, the movable block is displaced forward or backward to change the height of the step from h to

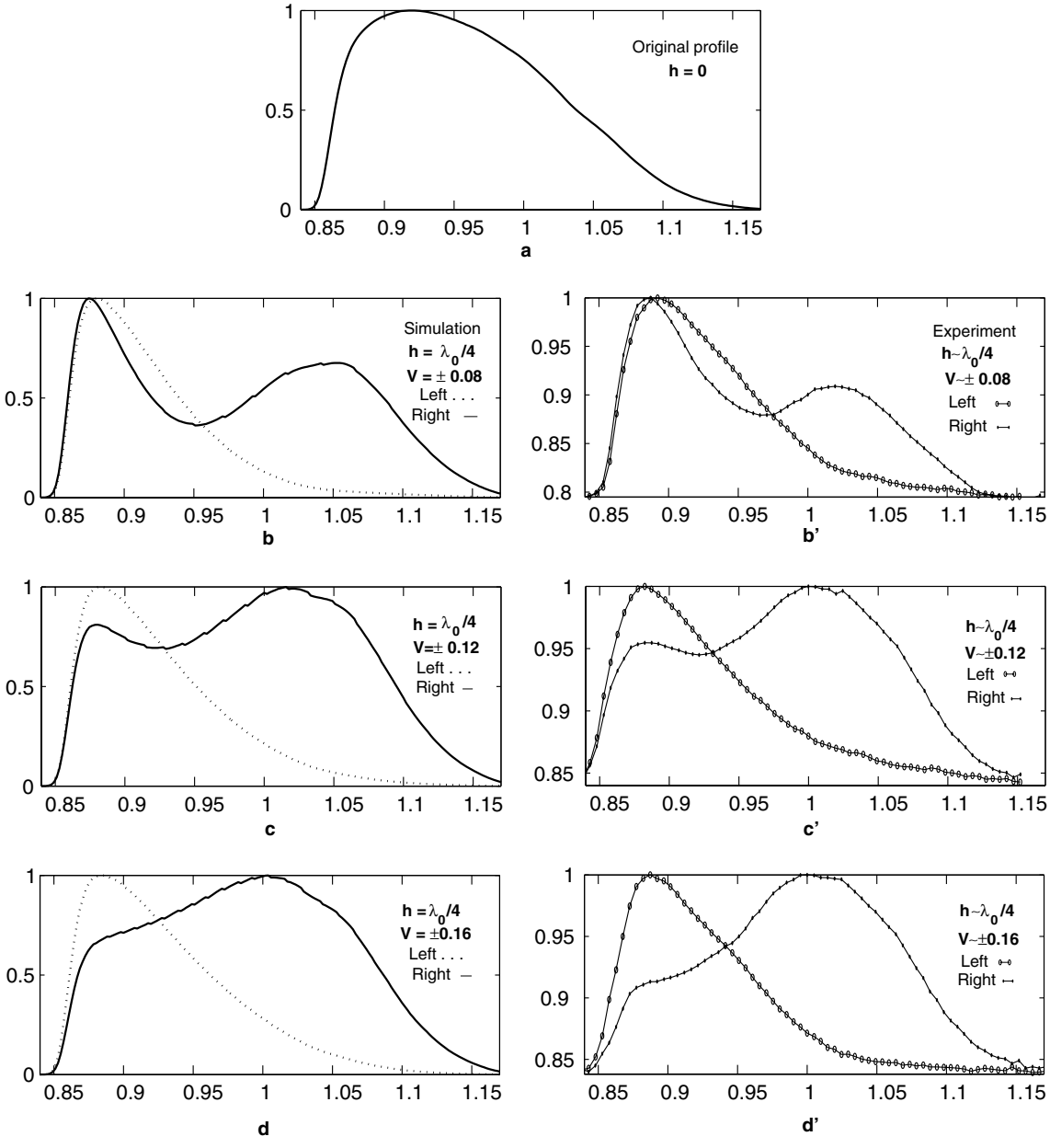

Fig. 3. (a) The normalized spectral profile of the filtered light source used in simulation and experimental studies of the spectral profiles of the light diffracted from a 1D phase step of height $h = \lambda_0/4$ ($\lambda_0 = 510$ nm), the line singularity, at different distances from the singularity, the step edge. (b), (c), and (d) show the simulations of the modified spectral profiles of the diffracted lights at normalized distances $v = \pm 0.08$, $v = \pm 0.12$, and $v = \pm 0.16$ from the step edge, respectively. (b′), (c′), and (d′) show the corresponding experimental profiles.

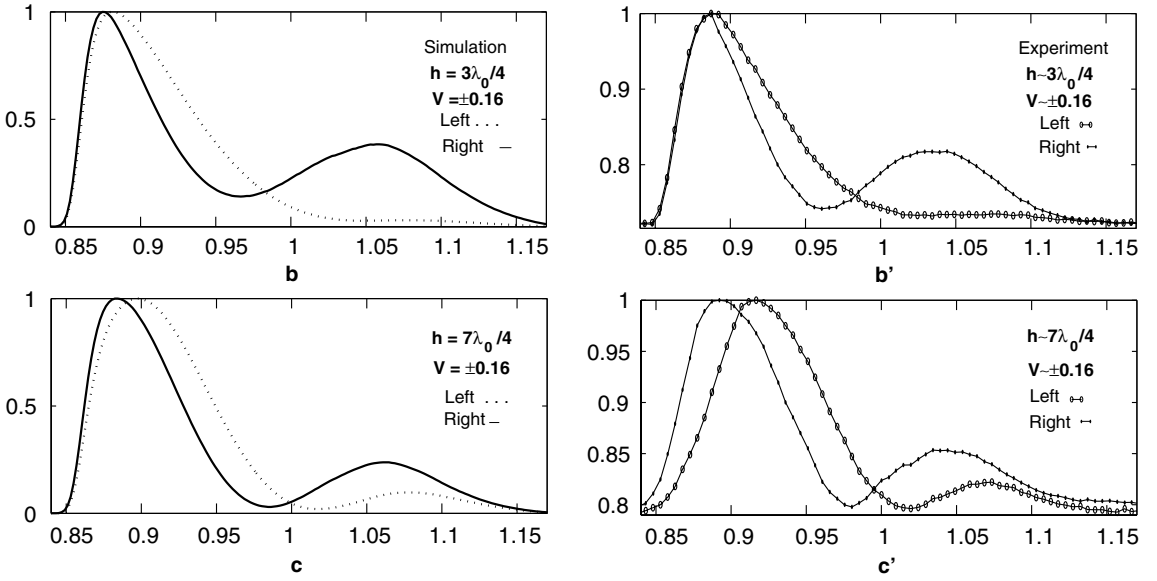

Fig. 4. (b) and (c) show the simulations of the modified spectral profiles of the lights diffracted from 1D phase steps of heights $h = 3\lambda_0/4$, and $7\lambda_0/4$, at normalized distances $v = \pm 0.16$ from the step edge. The light source profile is given in Fig. 3(a). Fig. 4(b′) and (c′) show the corresponding experimental profiles of the diffracted lights.

$-h$ or vice versa. This prevents misalignment and errors which are inevitable in displacing MC.

In order to compare the experimental results with the theoretical predictions, for each experiment, that is; for every experimental step height h and normalized distance v from the step edge, we use the spectral profile of the beam reflected from one of the blocks and the modifying factors, Eqs. (21) and (22), to simulate the corresponding diffracted spectral profile. The simulation procedure is as follows. For a given distance from the step edge x_0 and wavelength λ, the corresponding v_0, C, S, and M given by Eqs. (9), (15), and (21) or (22) are evaluated. Then, the resulted M is multiplied by the corresponding normalized spectral intensity taken from the experimental spectral profile. Then this procedure is repeated at 5 nm interval to cover the entire source spectrum.

The results of the experiments and the simulations are illustrated by the graphs in the following figures. In Fig. 3(a), the normalized spectral profile of the filtered source versus λ/λ_0, ($\lambda_0 = 510$ nm) is plotted. We refer to it as original or $h = 0$ profile. Fig. 3(b), (c), and (d) show the simulations of the modified spectral profiles of the lights diffracted from a 1D phase step of height $h = \lambda_0/4$, singularity for λ_0, at different distances from the singularity, the step edge. The distances on the right and the left sides of the step edge,[1] converted into normalized distances of the Cornu spiral for λ_0, are $v = \pm 0.08$, $v = \pm 0.12$, and $v = \pm 0.16$, respectively. The conversion ratio from millimeter to the normalized distance v is $\sim$1.49. The corresponding modified experimental profiles of the lights diffracted from similar phase steps are given in Fig. 3(b′), (c′), and (d′), respectively. The experimental and simulated profiles are quite similar. Some minor differences are inevitable because, the simulation curves deal with spectra at points; while in practice the width of MC's slit is finite and the effect becomes pronounced as we approach the singularity. As one can see in the graphs of Fig. 3 the left side and the right side profiles are quite different, and they also differ considerably from the original profile (Fig. 3(a)). The

[1] In Fig. 2, the step edge is a horizontal plane and it seems more sensible to use up-side and down-side of the edge, but, we have used left side and right side because of Fig. 1 and the Cornu spiral.

circles and dots are experimental points. The profiles in Fig. 3 show that modification depends on the distance from the singularity. Further experimental and simulation studies reveal that the difference between the left side and the right side profiles is small for the points very close to the singularity, $|v| < 0.04$, but, grows with the distance from the singularity up to $|v| \simeq 0.3$, and then decreases. These are consistent with Eqs. (21) and (22) that predict the modifying factors M_R and M_L are equal for small C and S, also for $C = S$, but, are different for $C \neq S$. In Fig. 4 we have plot-

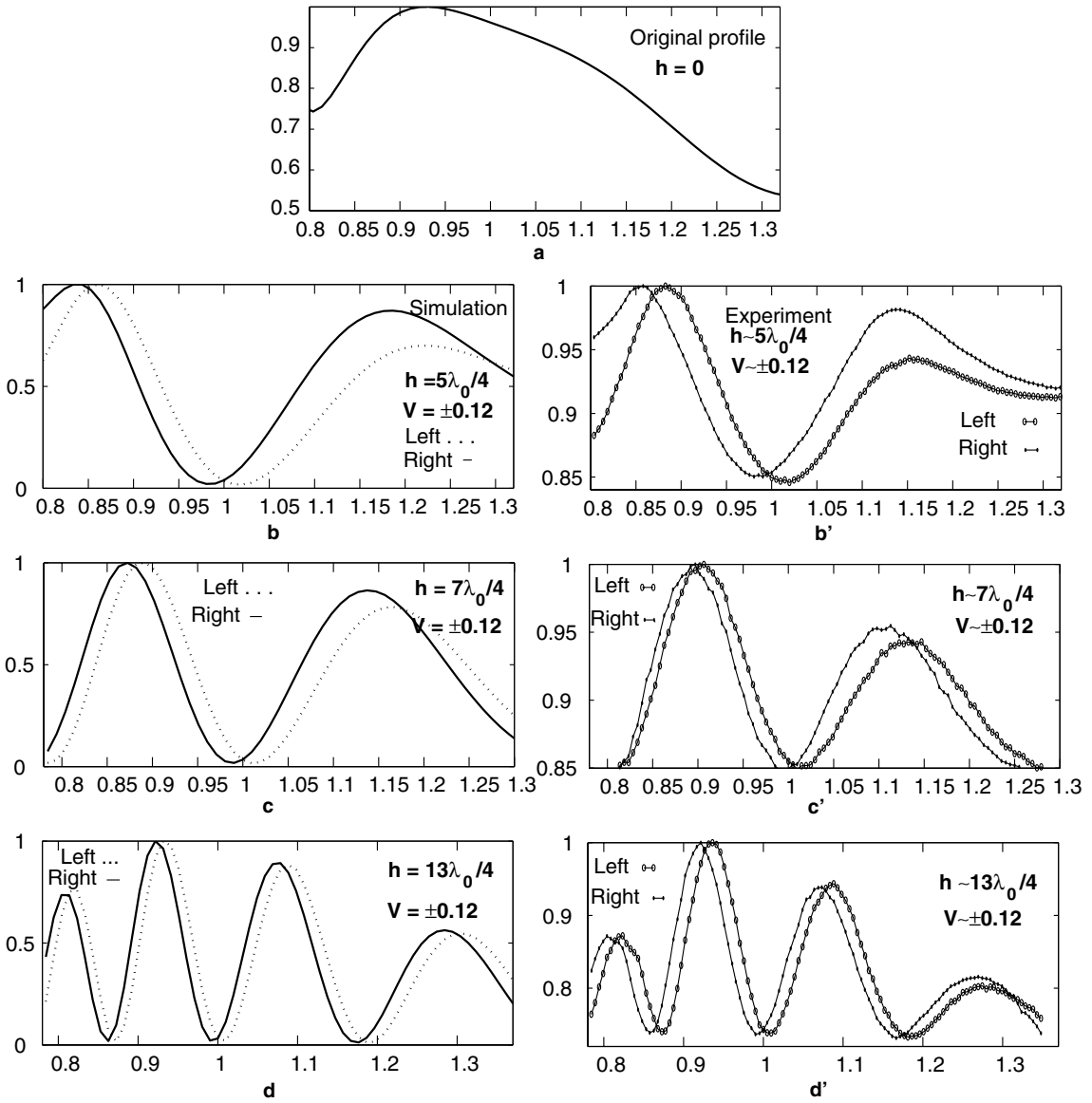

Fig. 5. (a) The normalized spectral profiles of the white light source versus λ/λ_0 ($\lambda_0 = 510$ nm), used in simulation and experimental studies of the spectral profiles of the light diffracted from 1D phase steps of different heights. (b), (c), and (d) show the simulations of the modified spectral profiles for the step heights $h = 5\lambda_0/5$, $h = 7\lambda_0/4$, and $h = 13\lambda_0/4$, respectively, at normalized distances $v = \pm 0.12$ from the step edge. The plots in (b′), (c′), and (d′) show the corresponding modified experimental profiles.

ted the modified simulated and the experimental spectral profiles for $h = 3\lambda_0/4$ and $7\lambda_0/4$ at the normalized distances $v = \pm 0.16$. Comparing these profiles with the profiles plotted in Fig. 3, we notice that the order of step height is effective in modification. More detail studies show that the difference between the left and the right profiles at relatively large distance from singularity is more pronounced for the higher step heights than for the lower ones. As the height of the phase step approaches to the coherent length of the source, the difference between the left and the right modifying factors vanishes.

In the second series of the experiments we just removed the filters and used the white light source described at the beginning of this Section. Some very interesting colorful features are observed. Beautiful colors with different hues appear at different singularities. The colors varies very sharply by variation of the step height and the gap between the two building blocks of the phase step. Even a gap of few micrometers can affect considerably. The colors change rapidly by the distance between the phase step and the observing point. But, the general behaviors of the modified spectrum are similar to those of the previous source. In Fig. 5 we have plotted the spectral profiles of the source, (a), and its corresponding modified simulated and experimental profiles, for the step heights $h = 5\lambda_0/4$, $7\lambda_0/4$ and $13\lambda_0/4$ at the normalized distances $v = \pm 0.12$ from the singularities. Here also the experimental and simulated profiles are quite similar and a clear shift between the right side and the left side profiles are observed. The dependence of the profiles on the step height for the same distance from the singularity is clear.

In Fig. 6, we have a color picture recorded by CCD from a spatially coherent beam of white light diffracted from a 1D phase step of height $h \simeq 130$ nm. The singularity and the observation planes intersect each other at the region between the blue and the orange strips. The colors on the both sides of the singularity are not symmetrical. The white strip, specified by an arrow, on the upper part of the picture, which is located over the lower part of the step is a region of zero optical path difference. The appearance of these white, blue and orange strips in the singularity region are in agreement with Berry's prediction [6]. By increasing the step height the white strip moves away from the singularity and disappears (Fig. 7). Also, Fig. 7 shows that the brightness of the colors on the both sides of the singularity is not the same. Another note worthy point is that as the height of the step approaches to zero, we expect to observe a uniform white light on the screen. But, usually we observe something similar to that is shown in Fig. 8, which

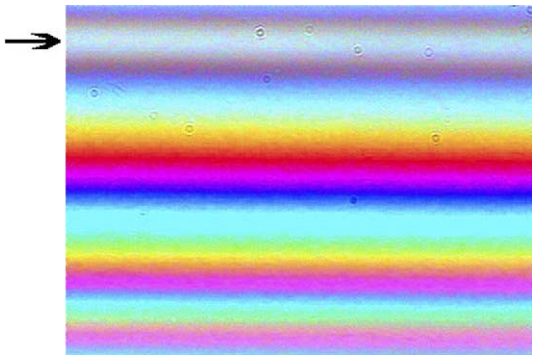

Fig. 6. The colored intensity distribution recorded by CCD of a white light beam diffracted from a 1D phase step of the height $h \approx \lambda_0/4$. The detector distance from the phase step was 100 cm. The white strip, specified by an arrow, on the upper part of the picture is the locus of zero optical path difference in the neighborhood of the singularity.

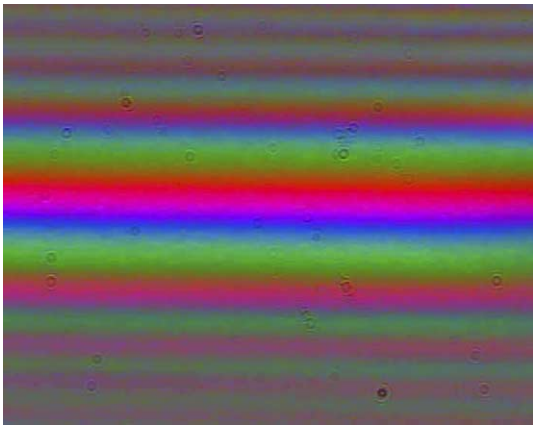

Fig. 7. The colored intensity distribution of a white light beam diffracted from a 1D phase step of the height $h \approx 3\lambda_0/4$ recorded by CCD. The detector distance from the phase step was 100 cm. The white strip in Fig. 6 has disappeared and the visibilities on both sides of the singularity are not the same.

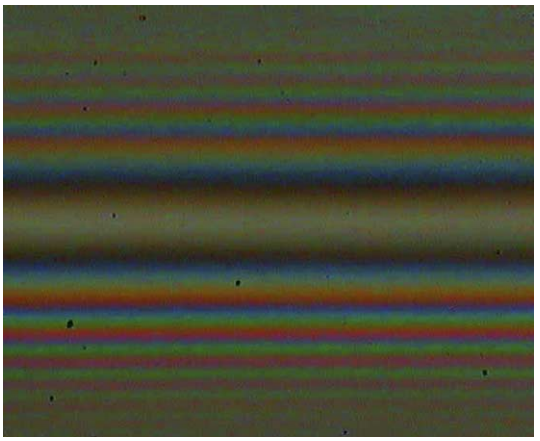

Fig. 8. The colored intensity distribution recorded by CCD of a white light beam diffracted from a 1D phase step of the height $h \simeq 0$. The appearance of symmetrical colored strips with a white strip at the middle is due to the bluntness of the edges of the blocks forming the phase step (see the context).

includes practically symmetrical colored strips, with a white strip at the middle of two black strips. This is because the edges of the blocks can not be very sharp, therefore, for $h = 0$, there is a dip between them, as is shown in Fig. 9. The optical path difference on the symmetry plane is zero, this leads to the white strip at the middle and symmetrical colored strips on both sides. In fact, the step behaves like an opaque strip. The colored strips shown in Fig. 10 belongs to the case that the step height is larger than the coherence length. There is a dark strip with symmetrical colored strips on both sides. In fact, in this case we have two independent semi-infinite reflecting surfaces which produce edge fringes on their bright regions.

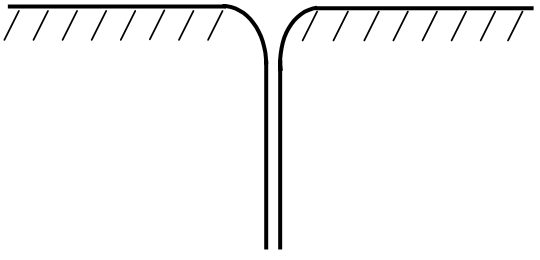

Fig. 9. The sketch of the phase step for $h = 0$. The bluntness at the edges of the blocks and the gap between them lead to nonuniform intensity distribution even at $h = 0$.

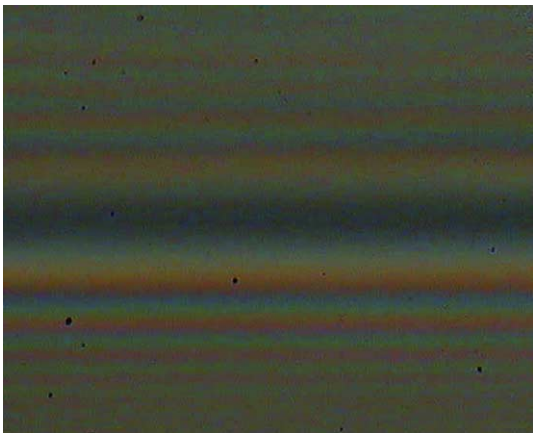

Fig. 10. The colored intensity distribution of a white beam light diffracted from a 1D phase step of the height greater than the coherence length.

4. Conclusions

Fresnel diffraction of a spatially coherent polychromatic beam of light from a 1D phase step, which provides line singularity, is studied. This kind of diffraction modifies the incident light spectrum remarkably and the modifying factor depends on the step height and the distance from the step edge. The modifying factor varies acutely in the neighborhood of the singularity. But, there are some serious obstacles to study the diffracted field in very close neighborhood of the singularity, namely, the finite size of the monochromator's entrance slit, the bluntness of the blocks' edges, and the limitations in arrangement prevent experimenter to approach singularity.

This kind of study not only provides a better understanding of diffracted fields and singular optics, but, it can have applications in producing diffractive optical elements (DOEs), in integrated optoelectronic circuits (IOCs), in coherent light imaging and so on [11–13]. The study can be extended to 2D's phase steps, to partially coherent illumination cases, and to steps with phase gradient at edges. Besides, it seems feasible that by studying the intensity distribution in the neighborhoods of different singularities one can specify the spectral profiles of the polychromatic lights.

Acknowledgments

The authors sincerely acknowledge the assistance provided by S.N.S. Reihani in instrumentation and data processing.

Appendix A. Inclination factor for cylindrical wave

In deriving the inclination factor $K(\gamma) = -\frac{i}{\lambda}$ for a spherical wave, in paraxial approximation, the result of the Fresnel–Kirchhoff integral

$$U(P) = \int\int_{\Sigma} AK(\gamma)\frac{e^{ik(R+r)}}{Rr}\,da, \tag{A.1}$$

is equated by the amplitude of the wave directly propagating from point S to point P [14] (Fig. A.1).

Now we apply the same approach to a cylindrical wave originating from a linear source perpendicular to the page at point S. For a cylindrical wave the amplitude at a distance R from the source can be given by $A/\sqrt{R}$. Thus, considering Fig. A.1, the Fresnel–Kirchhoff integral for a cylindrical wave can be expressed by

$$U(P) = \int_{\Sigma} AK(\gamma)\frac{e^{ik(R+r)}}{\sqrt{R}\sqrt{r}}\,d\rho, \tag{A.2}$$

where $d\rho$ is a line element on the cylindrical wave at point M. In paraxial approximation i.e., for a small θ, we have

$$r^2 = R^2 + (R+R')^2 - 2R(R+R')\left(1-\frac{\theta^2}{2}\right). \tag{A.3}$$

Now, substituting θ by ρ/R, where $\rho = \widehat{OM}$, and considering that $|\rho| \ll R$, Eq. (A.2) can be expressed as follows:

$$U(P) = \frac{KAe^{ik(R+R')}}{\sqrt{RR'}}\int_{-\infty}^{+\infty} e^{ik\left(\frac{R+R'}{2RR'}\right)\rho^2}\,d\rho. \tag{A.4}$$

Now, substituting ρ by v, which is defined as follows:

$$v = \rho\sqrt{\frac{2(R+R')}{\lambda RR'}}, \tag{A.5}$$

we get

$$U(P) = K\sqrt{\frac{\lambda}{2}}\frac{Ae^{ik(R+R')}}{\sqrt{R+R'}}\int_{-\infty}^{+\infty} e^{i\frac{\pi v^2}{2}}\,dv. \tag{A.6}$$

Recalling that

$$\int_{-\infty}^{+\infty} e^{i\frac{\pi v^2}{2}}\,dv = (1+i) \tag{A.7}$$

and

$$U(P) = \frac{Ae^{ik(R+R')}}{\sqrt{R+R'}}, \tag{A.8}$$

Eq. (A.6) leads to

$$K\sqrt{\lambda}e^{i\frac{\pi}{4}} = 1, \tag{A.9}$$

or

$$K = \sqrt{\frac{-i}{\lambda}}. \tag{A.10}$$

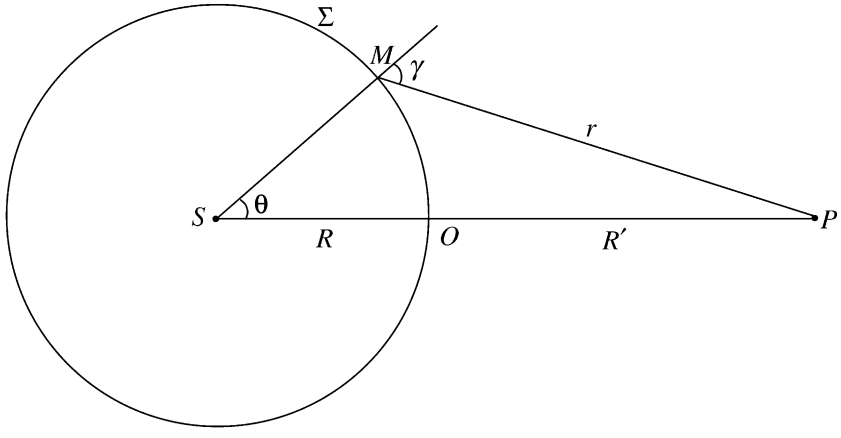

Fig. A.1. A profile of a cylindrical wavefront used for calculation of the inclination factor.

References

[1] J.F. Nye, Natural focusing and the fine structure of light, IOP, Bristol, 1999.
[2] M. Born, E. Wolf, Principles of Optics, seventh ed., Cambridge University Press, Cambridge, England, 1999 (Section 8.8.4).
[3] M.S. Soskin, M.V. Vasnetsov, in: E. Wolf (Ed.), Progress in Optics, 42, Elsevier, Amsterdam, 2001, p. 219.
[4] G. Gbur, T.D. Visser, E. Wolf, Phys. Rev. Lett. 88 (2001) 013901.
[5] G. Gbur, T.D. Visser, E. Wolf, J. Opt. Soc. Am. A 19 (2002) 1694.
[6] M.V. Berry, New J. Phys. 4 (2002) 66.1.
[7] M.V. Berry, New J. Phys. 4 (2002) 74.1.
[8] T.D. Visser, E. Wolf, J. Opt. A: Pure Appl. Opt. 5 (2003) 371.
[9] G. Popescu, A. Dogariu, Phys. Rev. Lett. 88 (2002) 183902.
[10] M. Born, E. Wolf, Principles of Optics, seventh ed., Cambridge University Press, Cambridge, England, 1999 (Section 8.7.2).
[11] H.H. Hopkins, J. Opt. Soc. Am. 69 (1979) 4.
[12] G. Bouwhuis, J. Braat, A. Huijser, J. Pasman, G. van Rosmalen, K. Schouhamer Immink, Principles of Optical Disk Systems, Hilger, London, 1985.
[13] T. Wilson, C. Sheppard, Theory and Practice of Scanning Optical Microscopy, Academic, New York, 1984.
[14] M. Born, E. Wolf, Principles of Optics, seventh ed., Cambridge University Press, Cambridge, England, 1999 (Section 8.8.2).